

HNPS Advances in Nuclear Physics

Vol 16 (2008)

HNPS2008



Search for exotic nuclear breakup configurations in Au+Au collisions

A. Sochocka, A. Benisz, P. Hachaj, N. G. Nicolis, R. Planeta, Z. Strypan

doi: [10.12681/hnps.2593](https://doi.org/10.12681/hnps.2593)

To cite this article:

Sochocka, A., Benisz, A., Hachaj, P., Nicolis, N. G., Planeta, R., & Strypan, Z. (2020). Search for exotic nuclear breakup configurations in Au+Au collisions. *HNPS Advances in Nuclear Physics*, 16, 155–163. <https://doi.org/10.12681/hnps.2593>

Search for exotic nuclear breakup configurations in Au+Au collisions

A. Sochocka^a, A. Benisz^b, P. Hachaj^c, **N.G. Nicolis^d**,

R. Płaneta^a and Z. Sarypan^a

^aM.Smoluchowski Institute of Physics, Jagiellonian University, Krakow, Poland

^bInstitute of Physics, University of Silesia, Katowice, Poland

^cCracow University of Technology, Krakow, Poland

^dDepartment of Physics, The University of Ioannina, Ioannina 45110, Greece

Abstract

We study the feasibility of an experimental observation of toroidal breakup configurations in $Au+Au$ collisions using the CHIMERA multidetector system. BUU simulations performed on the $^{197}Au+^{197}Au$ and $^{124}Sn+^{124}Sn$ systems indicate that the threshold energy for toroidal configuration formation decreases with increasing mass of the interacting system. For $Au+Au$ collisions, this threshold energy is found around 20 MeV/nucleon. Static model simulations are also employed in order to explore the nature of reaction events involving a toroidal breakup configuration.

The existence of nuclei with non-spherical shapes was first suggested by J.A. Wheeler [1,2]. This idea was investigated by many authors who studied the stability of exotic nuclear shapes and examined the possibility of their realization in nuclear collisions with dynamical model calculations. Siemens and Bethe showed that some bubble nuclei with sufficiently large charge may be stable against breathing deformation (monopole oscillations) [3]. Later, Wong showed that as nuclear temperature increases the surface tension coefficient decreases and the Coulomb repulsion is pushing nuclear matter outwards leading to the formation of exotic nuclei [4]. Stability of nuclear bubbles was also discussed by Moretto et al. [5].

Theoretical investigations related with the synthesis of long-living nuclei beyond the island of stability have shown that they can be reached only if non-compact shapes are taken into account. Calculations done for bubble structures with the liquid drop

model with shell corrections [6,7] and the HFB theory with the Gogny D1S force [8-10] show that bubble nuclei can be stable for $Z > 240$ and $N > 500$.

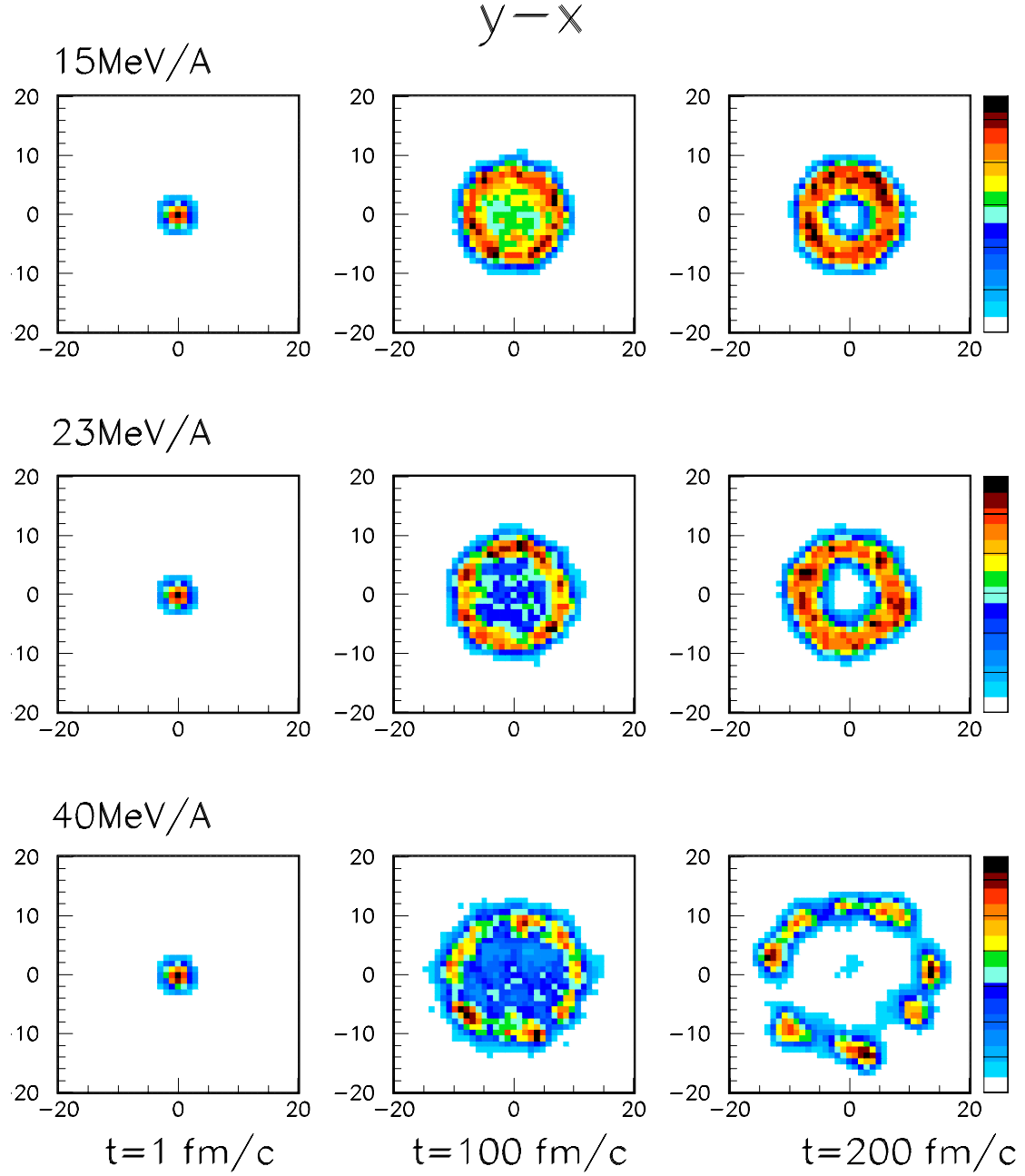
Recently the axially symmetric toroidal structure of super-heavy nuclei with $Z > 130$ has been analysed in frame of the HFB theory with Gogny D1S force. It was found that for nuclei with $Z > 140$ the global energy minimum corresponds to the toroidal shapes [11]. In contrast to bubble nuclei, the synthesis of toroidal nuclei could be experimentally available in the collisions of stable isotopes. The crucial issue is the selection of the colliding nuclei and collision energy.

To address this issue it is necessary to perform calculations with dynamical models. Already performed simulations using the BNV and BUU transport equations show that disc, bubbles, and toroidal shapes may be created in central and semi-central collisions. Such simulation were done mostly for systems with $A_{\text{sys}} < 200$ and they cover a large range of collision energies (60 - 100 MeV/nucleon) [12-18]. For heavier systems, such simulations are limited to $^{155}\text{Gd} + ^{238}\text{U}$ system at 27 and 35 MeV/nucleon [19] and $^{208}\text{Pb} + ^{197}\text{Au}$ at 20 to 55 MeV/nucleon [20].

A number of observables were suggested as the signatures of non-compact nuclear systems decay. These were: (i) more of intermediate mass fragments should be generated than would be expected for the decay of a compact object; (ii) enhanced similarity in the charge and size of the fragments should also be observed; (iii) suppressed sphericity in the emission of fragments should be visible.

In the following, we present results of dynamical and static model simulations performed for $\text{Au} + \text{Au}$ collisions in a wide range of incident energies. Dynamical simulations were performed with the BUU model. The static model calculations were performed using the ETNA code [21].

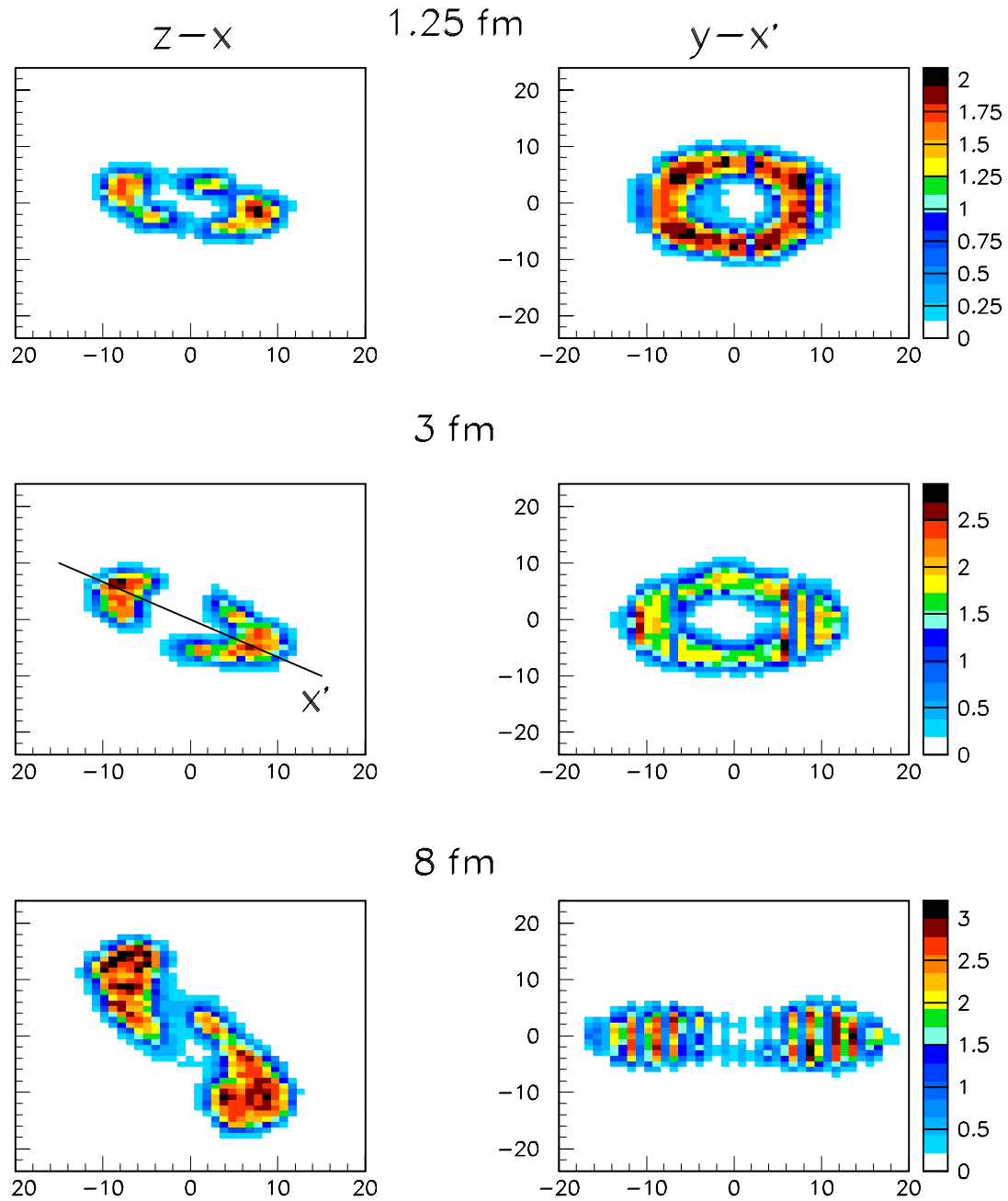
In our simulations the BUU code developed by Bao An Li is used [18]. The BUU equation is solved using the test - particle method. The number of test particles is equal 200, a cell size is 1 fm, a time step is 0.2 fm/c. The simulations were performed for time up to $t = 250$ fm/c. Calculations were done for two values of incompressibility parameter $K = 200$ MeV and 380 MeV. Two values of curvature parameter of symmetry energy $K_{\text{sym}} = -69 \text{ MeV}$ and 61 MeV were also used in our calculations.



(Color online) BUU calculations for central collisions of Au + Au at 15, 23, and 40 MeV/nucleon for $K = 200$ MeV. A time evolution in the x and y plane (cuts of the density distribution for $z = 0$, z axis - beam direction) is presented.

Fig. 1 shows the time evolution for Au + Au central collisions at 15, 23 and 40 MeV/nucleon for $K = 200$ MeV. Here nuclear matter density distributions in the x and y plane for $z = 0$ (z axis - beam direction) presented. One can observe that after the initial contact of the target and projectile, the nuclear matter is compressed to high density. This is followed by expansion mainly in the transverse direction. At the lowest energy the system reach the shape of a bubble contracted in the beam direction. At energy of 23 MeV/nucleon the system evolves to an oblate bubble

nuclear matter, which subsequently changes into ring-shaped structure. At the highest the radial expansion of the system is stronger. The oblate bubble shape is contracted in the z direction at the time of 100 fm/c and finally one observes several separated fragments arranged in the toroidal structure.



(Color online) Nuclear matter density distributions at 200 fm/c for $Au + Au$ at 23 MeV/nucleon ($K = 200$ MeV) for indicated values of impact parameter.

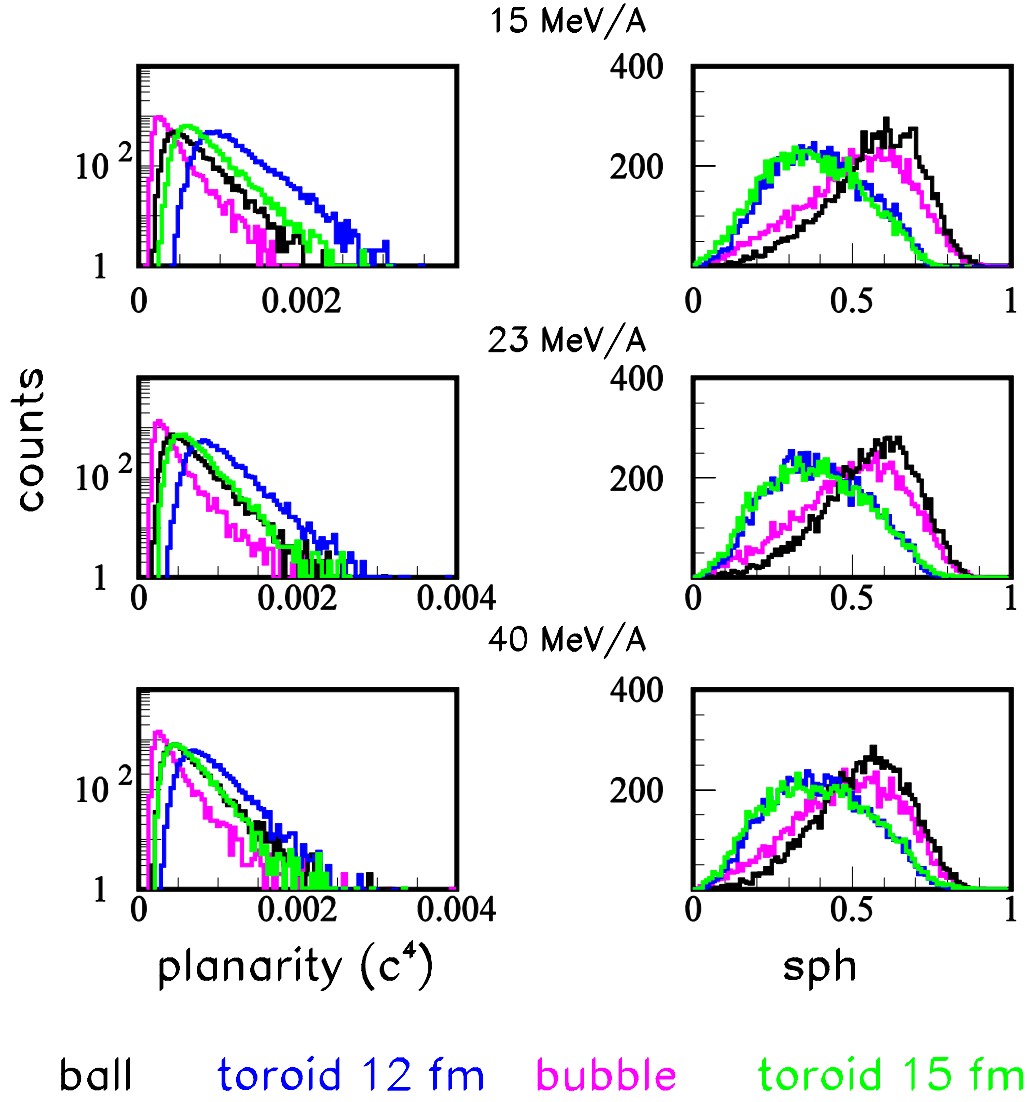
The left panels show an evolution in the x and z plane (cuts of the density distribution for $y = 0$, z axis - beam direction), the right panels show an evolution in the x' and y plane (for details see text).

Toroidal shapes are predicted also for semi-central collisions. Fig. 2 shows a nuclear matter density distribution at 200 fm/c for Au + Au collisions at energy 23 MeV/nucleon for impact parameters $b=1.25, 3$ and 8 fm. As can be seen in left panels the symmetry axes of the created toroidal objects are tilted away from the beam axis. This is a consequence of rotational motion for nonzero values of angular momentum. In the right panel the evolution after rotation about the y axis is presented. The x' axis is perpendicular to the symmetry axis of the tilted object. We observe that the toroidal object is formed for $b=1.25$ and 3 fm. This situation is kept for impact parameter below 7 fm. For impact parameters larger than about 7 fm, the residual systems assume stretched configurations leading to binary exit channels possibly accompanied by neck emission.

In order to test the applicability of CHIMERA multidetector [22] for recognition of non-compact nuclear geometries we developed the Monte Carlo simulation code ETNA (**Ex**pecting **T**oroidal **N**uclear **A**gglomerations) [21]. This code allows us to simulate the decay of the nuclear system assuming exotic break-up geometries. The charges of fragments are drawn from a Gaussian distribution centered at the total charge of the system divided by number of fragments. Results presented in this paper were calculated assuming a number of fragments is equal to 5.

Selected fragments are put into freeze out configurations. Four configurations were considered: (i) ball geometry with a volume 8 times greater than normal nuclear volume; (ii) a distribution of the fragments on the surface of the above mentioned sphere, thus simulating a bubble configuration; (iii) a distribution of fragments on a ring with diameter 12 fm; (iv) a ring with diameter 15 fm. The second geometry resembles the geometry found for freeze-out configuration in the analysis performed for central collisions of Gd + U nuclei at 36 MeV/nucleon [23]. The third and the fourth geometries correspond to the theoretical predictions of Ref. [11].

The angular momenta of the created systems are drawn up to a limiting value corresponding to the impact parameter of 3 fm. Energy conservation is then considered. The excess energy is distributed between excitation energy of fragments and their thermal motion assuming equal temperature limit. In the next step fragments are accelerated in their mutual Coulomb field. Following that step, they are filtered by software replica of the CHIMERA detector [24]. In our filtering procedure granularity of the detector was taken into account. We also require that the kinetic energy of the detected fragments is greater than 1 MeV/nucleon.



(Color online) The planarity (left panels) and sphericity (right panels) distributions for the investigated geometries at 15, 23, and 40 MeV/nucleon.

In order to disentangle between different break up geometries we tested several observables. Here we present the ETNA predictions for sphericity variable used commonly in nuclear physics to describe the shape of events in the momentum space. The second variable planarity introduced in this analysis gives a measure of events flatness and is defined as

$$\frac{1}{8} \sum_{\substack{(i,j)(k,l) \\ i \neq j \neq k \neq l}} |(\vec{v}_i \times \vec{v}_j) \cdot (\vec{v}_k \times \vec{v}_l)|$$

where \vec{v}_i are the CM velocities of the detected fragments.

In Fig. 3 the planarity (left panels) and sphericity (right panels) for the Au + Au reactions for four considered freeze-out geometries are presented at 15, 23, and 40 MeV/nucleon incident energies. One can see here that the sphericity distributions for the ball and bubble configurations are very similar and different from the distributions corresponding to toroidal configurations. One can also notice that the difference decreases with increasing incident energy. The difference in planarity distributions can disentangle between the toroidal and bubble shapes. Distinction between ball and toroidal configurations is weaker.

Details of the calculations shown in the present paper have been published in Refs. [25,26].

Summarizing, we presented results of dynamical and static model simulations for $Au + Au$ collisions. The BUU calculations indicate that the threshold energy for toroidal nuclear shapes formation is located around 23 MeV/nucleon. The results of the ETNA code calculations performed for the same system indicate that the sensitivity of studies observables to the assumed geometries decreases with increasing incident energy. QMD calculations are in progress in order to obtain a better understanding of the investigated observables.

References

- [1] J.A.Wheeler, Nucleonic Notebook, (1950) unpublished.
- [2] R.E.Euwema, J.A.Wheeler unpublished.
- [3] P.J.Siemens, H.Bethe, Phys. Rev. Lett. **18** (1967) 704.
- [4] C.Y.Wong, Phys. Rev. Lett. **55**, (1985) 1973.
- [5] L.G.Moretto *et al.*, Phys. Rev. Lett. **78** (1997) 824.
- [6] K.Dietrich and K.Pomorski, Nucl. Phys. A**627** (1997) 175.
- [7] K.Dietrich and K.Pomorski, Phys. Rev. Lett. **80** (1998) 37.
- [8] J.Decharge *et al.*, Phys. Lett. B**451** (1999) 275.
- [9] J.F.Berger *et al.* Nucl. Phys. A**685** (2001) 1.
- [10] J.Decharge *et al.*, Nucl. Phys. A**716** (2003) 55.
- [11] M.Warda, Int. J. Mod. Phys. E**16** (2007) 452.
- [12] L.G.Moretto *et al.*, Phys. Rev. Lett. **69** (1992) 1884.
- [13] H.M.Xu *et al.*, Phys. Rev. C**48** (1993) 933.
- [14] H.M.Xu *et al.*, Phys. Rev. C**49** (1994) R1778.

- [15] D.O.Handzy *et al.*, Phys. Rev. C**51** (1995) 2237.
- [16] S.R.Souza and C.Ngo, Phys. Rev. C**48** (1993) R2555.
- [17] W.Bauer *et al.*, Phys. Rev. Lett. **69** (1992) 1888.
- [18] Lie-Wen Chen *et al.*, Phys. Rev. C**68** (2003) 014605.
- [19] B.Borderie *et al.*, Phys. Lett. B**302** (1993) 15.
- [20] B.Jouault *et al.*, Nucl. Phys. A**591** (1995) 497.
- [21] A.Sochocka *et al.*, in: Proc. of the IWM 2005, eds.: R.Bougault, A.Pagano, S.Pirrone, M.F.Rivet and F.Rizzo, Conf. Proc. Vol. 91, (Societa Italiana di Fisica, 2006).
- [22] A.Aiello *et al.*, Nucl. Phys., A**583** (1995) 461.
- [23] G.Tabacaru *et al.*, Nucl. Phys. A**764** (2006) 371.
- [24] W.Gawlikowicz, Report ZFGM-03-02, Jagiellonian University, Cracow, 2003.
- [25] A. Sochocka, R. Planeta, N.G. Nicolis, Acta Phys. Pol. **39**, 405(2008).
- [26] A. Sochocka, A. Benisz, P. Hachaj, N.G.Nicolis, R.Planeta and Z. Starypan, Int. Jour. Mod. Phys. E**17**, 190(2008).